Cells from the Immune System Generate Adult-Born Neurons in Crayfish

Jeanne L. Benton,[1] Rachel Kery,[1] Jingjing Li,[1] Chadanat Noonin,[2] Irene Söderhäll,[2,3,*] and Barbara S. Beltz[1,3,*]
[1]Neuroscience Program, Wellesley College, Wellesley, MA 02481, USA
[2]Department of Comparative Physiology, Uppsala University, SE-752 36 Uppsala, Sweden
[3]Co-senior author
*Correspondence: irene.soderhall@ebc.uu.se (I.S.), bbeltz@wellesley.edu (B.S.B.)
http://dx.doi.org/10.1016/j.devcel.2014.06.016

SUMMARY

Neurogenesis is an ongoing process in the brains of adult decapod crustaceans. However, the first-generation precursors that produce adult-born neurons, which reside in a neurogenic niche, are not self-renewing in crayfish and must be replenished. The source of these neuronal precursors is unknown. Here, we report that adult-born neurons in crayfish can be derived from hemocytes. Following adoptive transfer of 5-ethynyl-2′-deoxyuridine (EdU)-labeled hemocytes, labeled cells populate the neurogenic niche containing the first-generation neuronal precursors. Seven weeks after adoptive transfer, EdU-labeled cells are located in brain clusters 9 and 10 (where adult-born neurons differentiate) and express appropriate neurotransmitters. Moreover, the number of cells composing the neurogenic niche in crayfish is tightly correlated with total hemocyte counts (THCs) and can be manipulated by raising or lowering THC. These studies identify hemocytes as a source of adult-born neurons in crayfish and demonstrate that the immune system is a key contributor to adult neurogenesis.

INTRODUCTION

Communication between the nervous system and the peripheral immune system is becoming more and more evident in mammals as well as in invertebrates, and it is now recognized that the immune and nervous systems rely on constant interaction to maintain homeostasis (Evans et al., 2010; Ransohoff and Engelhardt, 2012; An et al., 2014). For example, nonmyelinating Schwann cells associated with the autonomic innervation of bone marrow contribute to the maintenance of the hematopoietic stem cell pool in mice (Yamazaki et al., 2011), and the peripheral nervous system provides a microenvironment important for "homing" of hematopoietic cells and regulating their survival and development in *Drosophila* larvae (Makhijani et al., 2011). The studies presented in this article reveal a similarly intimate relationship between the immune and nervous systems in freshwater crayfish (*Procambarus clarkii* and *Pacifastacus leniusculus*), where the production of neurons

continues throughout the organisms' lives (for review, see Beltz et al., 2011; Benton et al., 2013). Our prior studies have shown that hemocytes—cells that underlie innate immunity in these invertebrate organisms—are attracted to the neurogenic niche in the crayfish brain in vitro (Benton et al., 2011). The current work demonstrates that the hematopoietic system exerts multiple levels of control over adult neurogenesis in the crustacean brain. Most importantly, following adoptive transfer of labeled hemocytes, these cells invade the neurogenic niche and their descendants differentiate into neurons. These findings challenge the canonical view that the ectodermal origin of embryonic neural tissues is the only source of neurons in the brain of adult crustaceans.

Invertebrates lack oxygen-carrying erythrocytes and blood cells of the lymphoid lineage that participate in the adaptive immune response, but have a well-developed innate immune system in which hemocytes (blood cells) play a leading role. Freshwater crayfish, such as *Pacifasticus leniusculus* and *Procambarus clarkii*, live for up to 20 years and contain distinct hematopoietic tissues (Noonin et al., 2012; Chaves da Silva, 2013) that synthesize hemocytes throughout the animal's lifetime. Astakines, crustacean cytokines belonging to the prokineticin family, are necessary for the proliferation and release of hemocytes from hematopoietic tissues (Söderhäll et al., 2005; Lin et al., 2010). In vertebrates, prokineticins are involved in diverse functions, including circadian regulation, angiogenesis, and neurogenesis; adult neurogenesis in the olfactory bulb is dependent on prokineticin 2 signaling (Ng et al., 2005). The goals of the present work were to assess the contribution of the innate immune system to the maintenance of a neurogenic niche and to test the competence of hemocytes as precursors of adult-born neurons in the crustacean brain.

New neurons are generated and incorporated into circuits in the adult brains of many vertebrate and invertebrate organisms, including in the crayfish *P. clarkii* and *P. leniusculus*. In decapod crustaceans, new neurons are added to visual areas located in the eyestalks (Sullivan and Beltz, 2005a) and to two groups of neurons in the deutocerebrum, cell clusters 9 and 10 (Figure 1), which contain local and projection neurons in the olfactory and accessory lobe (multimodal) pathway (Schmidt and Harzsch, 1999; Sullivan and Beltz, 2005b). The precursor cell lineage producing adult-born neurons has been identified in *P. clarkii*. The first-generation precursors, which are functionally analogous to neural stem cells in mammals, are located in a niche that is loosely attached to the ventral surface of the brain, beneath the sheath that surrounds the brain. The niche lies on a blood

CrossMark
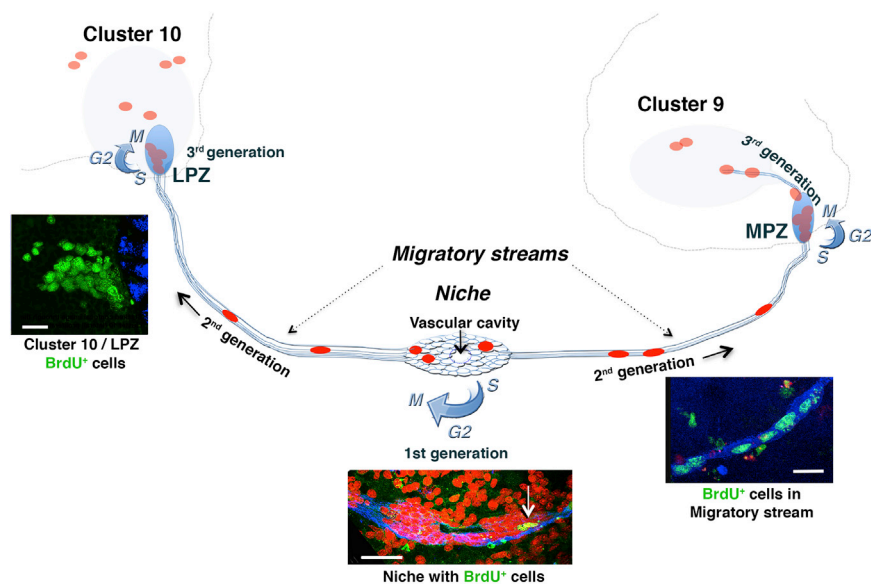
Figure 1. The Cellular Machinery Producing Adult-Born Neurons in the Crayfish Brain Consists of a Neurogenic Niche Containing First-Generation Precursors, Migratory Streams Containing Second-Generation Precursors, and Two Clusters of Olfactory Interneurons

The spatial relationships between these regions are indicated in the schematic drawing, which is supplemented with representative images of the niche, streams and cell clusters. In the diagram, BrdU-labeled (red) cells in the niche, streams and Cluster 10 are illustrated. First-generation precursors in a neurogenic niche divide symmetrically, both daughters migrating to proliferation zones (MPZ, LPZ) in Clusters 9 and 10, where they divide at least once more before progeny differentiate into neurons. Solid black arrows next to the streams indicate the direction of migration; curved, thick blue arrows indicate locations of cell divisions. The niche is connected to the blood system via a central "vascular cavity" in the niche, illustrated in the diagram and appearing as a white vacant region in the center of the niche image. In the accompanying images, BrdU (green) labeling is shown in each region of the niche-stream-cluster system. PI (red) labeling of all niche cell nuclei is also evident, as is the vascular cavity that appears as a black hole in the center of the niche. Glutamine synthetase immunoreactivity (blue) highlights the niche and streams. Scale bars represent 50 μm (niche); 20 μm (Cluster 10 and streams).

vessel (Sullivan et al., 2007), and in crustaceans such peripheral arterioles open into sinuses (i.e., hemolymph spaces that lack an endothelium, but that form narrow channels and broad lacunae within and around a tissue [Vogt, 2002]). The niche lies within this type of space and is therefore bathed in hemolymph, which also is funneled into the niche via the vascular cavity (Figure 1). However, the vascular cavity itself is not lined by an endothelium and therefore is not simply an extension of the blood vessel on which the niche lies (Chaves da Silva et al., 2012).

Unlike traditional stem cells, the first-generation neuronal precursors are not self-renewing, instead dividing symmetrically followed by the migration of both daughters away from the niche (Zhang et al., 2009). The absence of self-renewal has been unequivocally demonstrated using pulse-chase double-nucleoside labeling, which shows that the first-generation niche precursors do not retain the nucleoside label as would be expected if these divisions were self-renewing. Instead, following the niche cell divisions, the nucleoside is found exclusively in second-generation offspring that migrate in streams away from the niche (Benton et al., 2011). Rapid cycling of the niche precursors (and hence dilution of the BrdU label) cannot explain these results; 5–7 days are required for cells to traverse the migratory streams (the only sink for cells coming from the niche) (Sullivan et al., 2007), and there are no more than 12 cells in the streams at any time, indicating $\geq$48 hr cycle time (Benton et al., 2011).

The second-generation neuronal precursors migrate along fibrous streams formed by the processes of bipolar cells residing in the niche, until they reach proliferation zones in cell cluster 9 or 10 (Figure 1). There, they divide at least one more time before differentiating into neurons (Sullivan and Beltz, 2005a; Kim et al., 2014). Because of the spatial separation of the precursor lineage, each precursor generation can be examined independently (e.g., Zhang et al., 2011).

In spite of the fact that the first-generation neuronal precursors are not self-renewing, these precursors are never depleted and neurons continue to be generated throughout the animal's lifetime. The niche therefore cannot be a closed system. Thus, we have proposed that the pool of neuronal stem cells must be replenished from a source extrinsic to the niche. In vitro studies demonstrate that cells extracted from the hemolymph (but not other cell types) are attracted to the niche and that semigranular hemocytes have a particular affinity for the niche (Benton et al., 2011). These and additional studies (Sintoni et al., 2012; Chaves da Silva et al., 2012) suggest that the hematopoietic system may be one source of neuronal precursor cells in the neurogenic niche (Beltz et al., 2011).

In the present studies, we tested the relationship between the immune system and adult neurogenesis by manipulating the number of circulating hemocytes and subsequently assessing changes in the neurogenic niche containing the first-generation neuronal precursors. Astakine 1 (AST1) is known to specifically promote the proliferation and release of semigranular hemocytes in the crayfish *P. leniusculus* (Lin et al., 2010), and the present studies show that recombinant-AST1 (r-AST1) also promotes proliferation of the neuronal precursor lineage. When total hemocyte count (THC) was manipulated, THC and cell number in the neurogenic niche were positively correlated. Further, the reduction in niche cell number resulting from partial hematopoietic tissue (HPT) ablation was "rescued" by injection of r-AST1 prior to sacrifice. Finally, adoptive transfer of labeled hemocytes resulted in: (1) the integration of labeled cells into the neurogenic niche, (2) migration of labeled cells in the streams along which neuronal precursors travel, and (3) incorporation of labeled cells into brain clusters 9 and 10, where after several weeks they expressed neurotransmitters appropriate for these olfactory interneurons. Taken together, these studies demonstrate that the

innate immune system is directly involved in the production of adult-born neurons in the crayfish brain and indicate that neuronal precursors are derived from cells produced by the innate immune system.

RESULTS

AST1 Raises Total Hemocyte Counts in *P. clarkii*

To test whether hematopoietic tissues in *P. clarkii* are responsive to *P. leniusculus* r-AST1, this cytokine was injected into *P. clarkii*. Hemolymph samples were taken from crayfish at 6, 12, 18, 24, and 48 hr after injection, and for each individual crayfish the THC after injection was normalized to the initial hemocyte count at time 0, just prior to injection (Figure 2A). This and all subsequent experiments were conducted at room temperature so that temporal aspects of the various data sets could be compared. THC measured after r-AST1 injection shows variability in blood cell counts between same-size crayfish, even at time 0. However, at 12 hr postinjection, a significant increase in the THC occurs; THC returns to nearly preinjection levels by 18 hr postinjection. This experiment confirms that hematopoietic tissues in *P. clarkii* respond to r-AST1 and defines the time course of the hematopoietic response. In comparable experiments conducted at 10°C in *P. leniusculus*, the release of semigranular cells and corresponding change in total hemocyte counts occurs 24 hr after r-AST1 injection (Lin et al., 2010). This 12 hr difference in response time is likely due to the lower temperature used in the *P. leniusculus* study, as THC is highly affected by water temperature (Jiravanichpaisal et al., 2004).

The high variability in hemocyte counts in crustacean species is due to a variety of factors such as circadian phenomena (Watthanasurorot et al., 2011), temperature (Jiravanichpaisal et al., 2004), and diet (Stewart et al., 1967). The injection of even small amounts of fluid, the insertion of a needle to extract hemolymph, or any surgical procedure or infection alters circulating hemocyte number and can cause the release of AST1 and other factors into the plasma from activated hemocytes. This response is followed by a recovery accomplished primarily through the rapid synthesis and release from hematopoietic tissues (Söderhäll et al., 2003). Therefore, to ensure that multiple variables did not confound our results, hemolymph samples were not taken during the r-AST1 experiments described below.

R-AST1 Alters the Rate of BrdU Incorporation and Cell Number in the Niche

R-AST1 was injected into *P. clarkii*, and groups of crayfish (including normal controls [no treatment] and shams [injected with saline]) were then maintained in pond water containing 5-bromo-2′-deoxyuridine (BrdU). After sacrifice at 24, 48, and 72 hr postinjection, brains were dissected, processed immunocytochemically, and stained with propidium iodide (PI). The total number of cells in the niche (based on PI labeling) and BrdU-labeled cells in the niche, streams and Clusters 9 and 10 were counted. We then asked whether changes in the niche or precursor cell lineage were correlated with the release of hemocytes initiated by r-AST1 injection.

At 24 hr postinjection, no changes were observed in any of these regions (Figures 2B–2D). However, by 48 hr postinjection, the total numbers of cells (Figure 2B) and BrdU-labeled cells

in the niche (Figure 2C) increased relative to sham controls. At 72 hr postinjection, the increase in the number of niche cells was maintained, while the number of BrdU-positive cells returned to control levels. The migratory streams from the niche to Clusters 9 and 10 contain all of the cells migrating from the niche and these show an increase in BrdU-positive cells at 48 hr (Figure 2D), suggesting that the initial rise in BrdU-labeled niche cells actually occurred prior to the 48 hr time point, thus providing a window of time when the second-generation cells resulting from the division of niche cells could migrate into the streams; alternatively, r-AST1 could be directly accelerating the cell cycle among the second-generation precursors, which progress through the cell cycle and sometimes divide while in the streams (Sullivan et al., 2007). While Cluster 9 BrdU-labeled cell counts did not vary from controls or shams at any of the time points, in Cluster 10 there was an increase in the number of BrdU-labeled cells relative to shams at 72 hr (Figure S1 available online). Because migration from the niche to the proliferation zones normally requires 5-7 days (Sullivan et al., 2007), it is unlikely that the migration of cells into Cluster 10 can explain this result. Therefore, this influence on BrdU labeling in Cluster 10 indicates that r-AST1 directly affects neuronal precursor cells in this cluster, promoting their division.

We also examined the vascular cavity, located centrally in the niche, at each of the time points. Communication between the vascular cavity and the circulation has been demonstrated by injection of labeled dextran into the pericardial sinus (Benton et al., 2011) or into the dorsal median artery (Sullivan et al., 2007). The niche lies on a blood vessel, to which it is connected by a plexus of fine channels (Chaves da Silva et al., 2012). In control preparations, there is <10% chance of observing cells (detected with PI labeling) within the cavity (Figure 2E). Following r-AST1 injection, the incidence of finding cells in the cavity was unchanged at 24 hr, but increased sharply at 48 hr to 35% (Figure 2F). While still above control levels at 72 hr, the chance of observing a cell in the cavity dropped to <20%. These data suggest that between 24–48 hr following r-AST1 injection, cells find their way to the vascular cavity within the niche. The size and cytology of these cells suggests that these are hemocytes, which would have increased in the circulation by 12 hr following r-AST1 injection (Figure 2A).

Ablation of Hematopoietic Tissue Reduces the Numbers of Niche Cells, and r-AST1 Restores These Numbers to Sham Levels

We hypothesized that if the number of niche cells and neuronal precursors (BrdU-labeled cells in the niche) are indeed regulated by the hematopoietic system and by circulating hemocyte levels, then reducing the amount of hematopoietic tissue (HPT) should diminish the number of cells in the neurogenic niche. Indeed, ablating roughly half of the posterior HPT (Figure S2) resulted in a significant reduction in the number of niche cells after 7 days, to 68% of sham values (Figure 3A). However, if r-AST1 is injected into the half-ablated (HA) crayfish 48 hr prior to sacrifice, the number of niche cells is restored to sham levels. These experiments show that cell numbers in the neurogenic niche are readily and predictably altered by manipulation of the hematopoietic system, either by partial ablation of the HPT (decrease in niche cell numbers) or by the release of cells
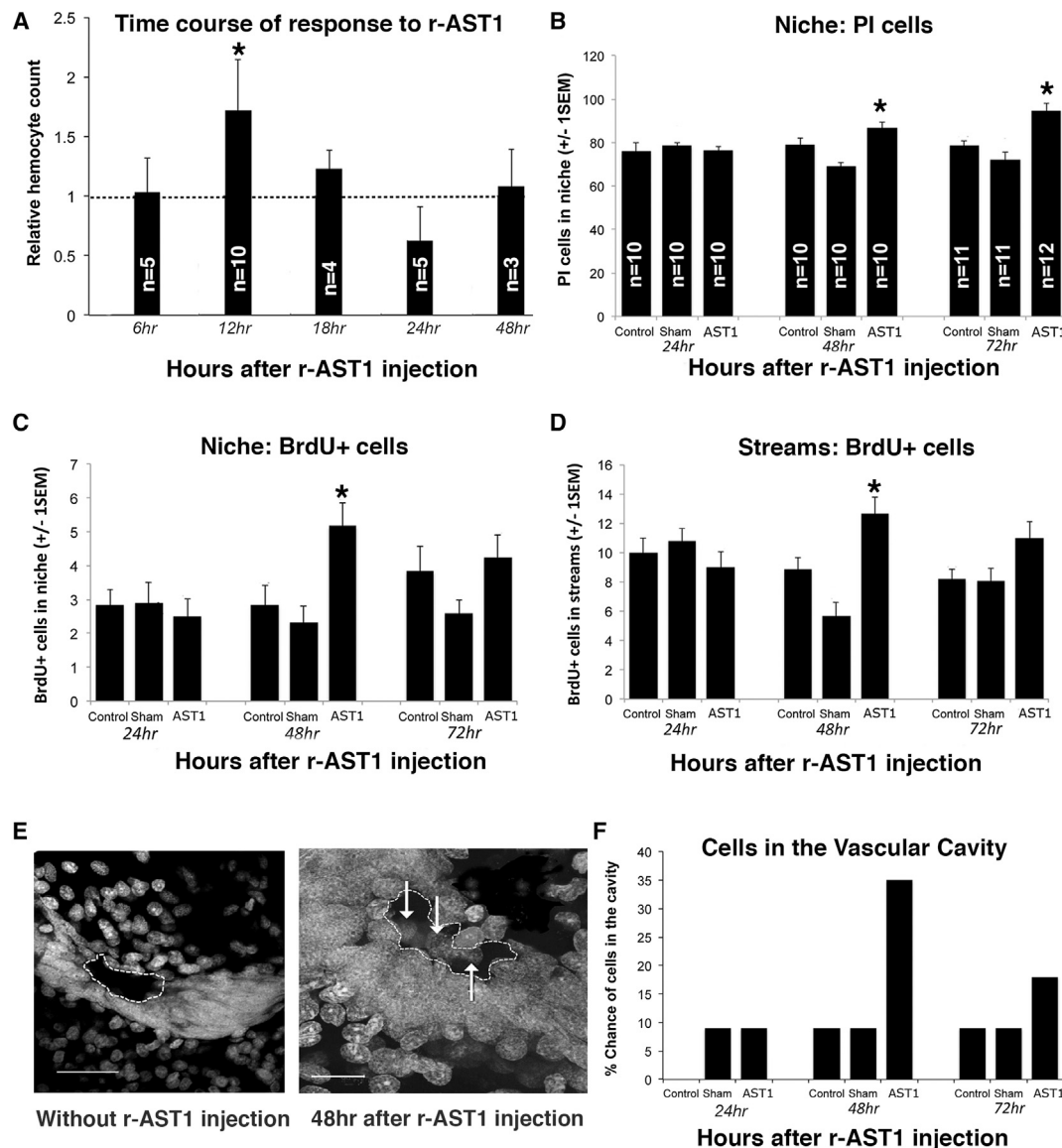
Figure 2. Injection of r-AST1 into Crayfish Promotes Hemocyte Release and Is Correlated with an Increase in the Number of First- and Second-Generation Neuronal Precursors

(A) Time course of hemocyte release after r-AST1 injection into *P. clarkii*. Total hemocyte counts (THC) were assessed at 6, 12, 18, 24, and 48 hr following r-AST1 injection into crayfish. The relative hemocyte count was calculated as the total number of hemocytes at each time point (black bars) divided by the hemocyte count just prior to r-AST1 injection (dashed line). These data show that the greatest release of hemocytes occurs 12 hr following r-AST1 injection (p = 0.0002). There also is a trend suggesting lower hemocyte levels 24 hr after injection (p = 0.06) and a return to control levels by 48 hr postinjection. N refers to the number of crayfish from which hemolymph samples were taken. Data are shown as means ± SEM. The asterisk above the 12-hr histogram indicates statistical significance (p ≤ 0.05) compared with other time points.

(B) The number of PI-labeled cells in the niche were counted in control, sham, and r-AST1-injected crayfish at 24, 48, and 72 hr after injection. Increases in mean niche cell counts relative to shams were observed at 48 (ANOVA, F = 2.30, p < 0.0002) and 72 (ANOVA, F = 2.30, p < 0.001) hr after r-AST1 injection. N indicates the number of niches that were counted. Data are shown as means ± SEM. Asterisks above histograms indicate statistical significance (p ≤ 0.05) compared with sham controls within each time period.

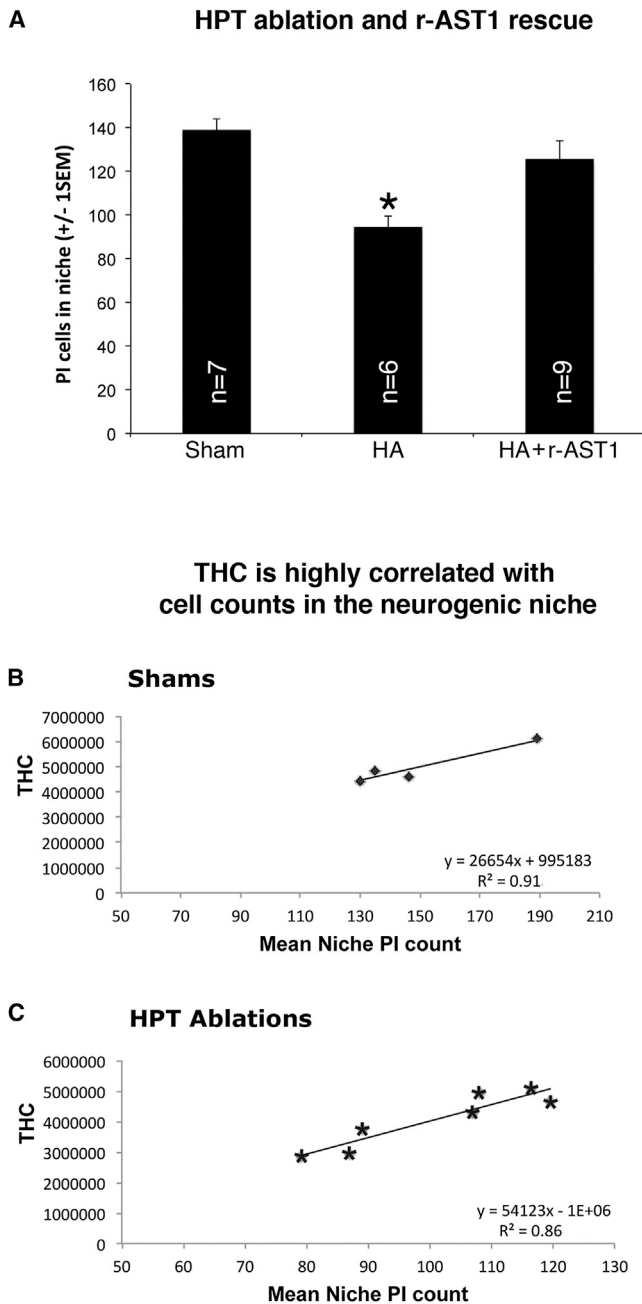(C and D) By 48 hr after r-AST1 injection, the numbers of BrdU-positive cells in the niche (C) and streams (D) increase transiently (C, ANOVA, F = 2.33, p < 0.004; D, ANOVA, F = 2.33, p < 0.0001). N indicates the number of niches that were counted. Data are shown as means ± SEM. Asterisks above histograms indicate statistical significance (p ≤ 0.05) compared with sham controls within each time period.

(E) Following r-AST1 injection, the chance of seeing cells in the vascular cavity increases. An image of a niche stained with the nuclear marker DAPI shows cells (arrows) located in the vascular cavity (dotted outline) in r-AST1-treated animals, while niches without r-AST1 treatment rarely have cells in the vascular cavity. Scale bar represents 20 μm.

(F) The chance of seeing cells in the vascular cavity following r-AST1 injection was quantified. Each histogram represents the mean of observations of ten or more niches (N values in B also apply to this graph). N indicates the number of niches that were counted.

See also Figure S1.

A HPT ablation and r-AST1 rescue

THC is highly correlated with cell counts in the neurogenic niche

B Shams

$$y = 26654x + 995183$$
$$R^2 = 0.91$$

C HPT Ablations

$$y = 54123x - 1E+06$$
$$R^2 = 0.86$$

Figure 3. The Number of Cells in the Neurogenic Niche Is Attenuated or Increased by Lowering or Raising Total Hemocyte Counts, Respectively

(A) The numbers of propidium iodide (PI)-labeled cells in the niche are reduced by partial ablation of posterior hematopoietic tissues. HPT-ablated crayfish (HA) have a significantly lower number of niche cells compared with shams that underwent partial surgeries but without the removal of any hematopoietic tissues (ANOVA, F = 2.19, p < 0.002). Injection of r-AST1 into HA crayfish 48 hr prior to sacrifice (HA+AST1) restores the niche cell counts to sham values. Data are shown as means ± SEM.

(B and C) Total hemocyte counts (THC) and mean niche cell (PI) counts are positively correlated, and the strength of the correlation is dependent on treatment group (shams, $R^2 = 0.92$; HPT ablated, $R^2 = 0.87$).

See also Figure S2.

following r-AST1 injection (restoration of niche cell numbers after ablation). The relatively brief time course of these experiments indicates that the size of the niche cell population is dynamically regulated by the hematopoietic system, consistent with the response of the niche and precursor cell lineage to r-AST1 injection (Figures 2B–2D). Because BrdU incorporation into niche cells was not altered by HPT ablation, cell divisions of the niche cells do not contribute to the change in total niche cell numbers.

As a control to test for generalized responses of proliferating tissues and overall health of the crayfish following HPT ablation, the hepatopancreas also was examined to ask whether BrdU labeling in this highly proliferative tissue was altered. No changes in the proportion of BrdU-labeled cells in this tissue were observed, indicating that cell proliferation in this organ was not altered by the HPT ablation. Taken together, these data suggest that the influence of hematopoietic tissue manipulation on the neurogenic niche is not part of a generalized response, but rather is a specific and localized effect. These results, as well as the normal behavior and activity of HA animals, also provide evidence that the surgeries did not adversely influence the health of the crayfish.

The Number of Cells in the Neurogenic Niche Is Correlated with Total Hemocyte Count

Based on the half-ablations of the HPT and r-AST1 rescue experiments (Figure 3A), we hypothesized that the number of niche cells is positively correlated with the total number of circulating hemocytes. In another experiment where hematopoietic tissues were ablated, niche cells and circulating hemocytes were counted. When sham and ablated animals are grouped together, the numbers of niche cells are positively correlated with THC ($R^2 = 0.74$). Such a strong correlation could be due to a common upstream regulatory factor influencing both THC and niche cell numbers. However, separating counts for sham and HPT-ablated animals reveals even stronger correlations between THC and niche cell numbers (shams, $R^2 = 0.92$, Figure 3B; HPT-ablated animals, $R^2 = 0.87$, Figure 3C). This increase in the strength of the correlation when sham and ablated animals are considered independently suggests that manipulation of hematopoietic tissues is responsible for the change in niche cell numbers. These studies are consistent with the hypothesis that niche cells are of hematopoietic origin, as proposed based on in vitro studies (Beltz et al., 2011).

A Source of Neuronal Precursors Is Extrinsic to the Niche

Prior studies have demonstrated that first-generation neuronal precursors in crayfish are not self-renewing and therefore must be replenished from a source extrinsic to the niche (Benton et al., 2011). The existence of such a source has been confirmed by studies in which adult crayfish were injected with BrdU. Labeling in the niche was then documented daily for 1 week and subsequently at intervals until 21 days after injection. The rationale for this experiment is that cells in S phase in all tissues will incorporate BrdU. First-generation precursors in the niche that are in S phase during the BrdU exposure period will be labeled, as will cells in tissues that are a source of neuronal precursors in the niche. However, we hypothesized
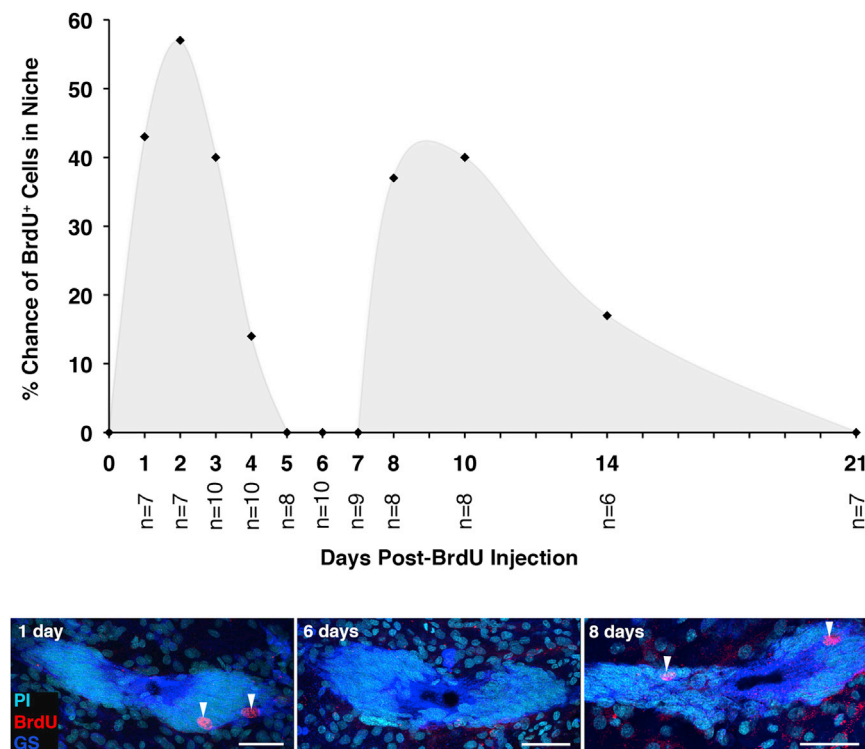
Figure 4. Actively Proliferating (BrdU-Labeled) Cells in the Neurogenic Niche Have a Bimodal Temporal Distribution

BrdU-labeled cells were quantified in the niches of crayfish that were sacrificed daily for 1 week after BrdU injection and at intervals thereafter for 21 days. The probability of observing BrdU-labeled cells in the niche was then plotted for each of the sampling days. BrdU-labeled cells are observed in the niche on days 1–4 following injection. On days 5–7, niches contain no BrdU-labeled cells. However, between days 8–14 after injection, BrdU+ cells are once again observed in the niche. Images of representative niches are included below the graph. PI, propidium iodide; GS, glutamine synthetase. Scale bars represent 50 μm.

fore, to further test this hypothesis, adoptive transfer methods were used to assess the competence of hemocytes as neuronal precursors in vivo. EdU, a nucleoside analog of thymidine that is incorporated into DNA during DNA synthesis, was injected into donor crayfish (*P. clarkii* and *P. leniusculus*) with the goal of labeling actively proliferating precursor cells in hematopoietic tissues, which will later release labeled hemocytes into the circulation. Blood was drawn from the donors 3–9 days later and transferred directly to recipient crayfish. EdU labeling of hemocytes was confirmed by direct examination of cells in the hemolymph being transferred. These transfers were done after the EdU clearing time and therefore EdU was not freely available in the transferred sample. EdU was used because the detection of this label does not require the use of antibodies that could bind nonspecifically. Instead, EdU incorporation is revealed by a copper-catalyzed covalent reaction between an alkyne (in the EdU) and an azide (in the Alexa Fluor dye). Thus, any EdU labeling observed in recipient crayfish must have originated in the transferred donor cells.

By 3 days posttransfer, EdU-labeled cells populate the neurogenic niche (Figure 5A). These cells are similar in size and morphology to other cells composing the niche and are immunoreactive for glutamine synthetase, as are other niche cells and precursors in the neuronal lineage in *P. clarkii*. EdU-labeled cells are observed in the migratory streams shortly thereafter (Figure 5B). Within 10 days of transfer, EdU-labeled cells are seen at the distal ends of the migratory streams (Figure 5C) and in cell clusters 9 and 10, where adult-born neurons differentiate. Finally, by 7 weeks after hemolymph transfer, the EdU-labeled cells in Clusters 9 and 10 of recipient crayfish express transmitters appropriate for these neuronal types (Figures 5D and 5E). In Cluster 9 (Figure 5D) the EdU-labeled cells contain immunoreactivity for orcokinin, while EdU-labeled cells in Cluster 10 are SIFamide-immunoreactive (Figure 5E) (Sullivan et al., 2007). These two peptide transmitters are characteristic of subsets of neurons in the respective neuronal clusters (Yasuda-Kamatani and Yasuda, 2006) and demonstrate that the

that cells labeled in the source tissue that are destined to become neuronal precursors will arrive at the niche after a delay, because of the time required to complete their lineages, be released and travel to the niche.

First-generation neuronal precursors in the niche (one to five cells) are reliably labeled with BrdU on days 1–4 following the exposure period (Figure 4), as shown in many previous studies (Sullivan et al., 2007). On days 5–7 after treatment, BrdU+ cells are no longer found in the niche because the BrdU <2-day clearing time (Benton et al., 2011) is over, and the originally-labeled cells have divided and exited the niche, migrating toward Clusters 9 and 10. However, on days 8–14 following BrdU exposure, intensely labeled cells are once again observed in the niche. As BrdU is no longer available for renewed labeling of neuronal precursors in the niche, our interpretation is that the "second wave" of labeled cells must have incorporated the nucleoside while still in their source tissue (Figure 4). Further, this bimodal curve of niche cell labeling following a single pulse of BrdU has also been documented in *P. leniusculus* (I.S. and B.S.B., unpublished data) and the hermit crab *Coenobita clypeatus* (S. Harzsch and B.S.B., unpublished data).
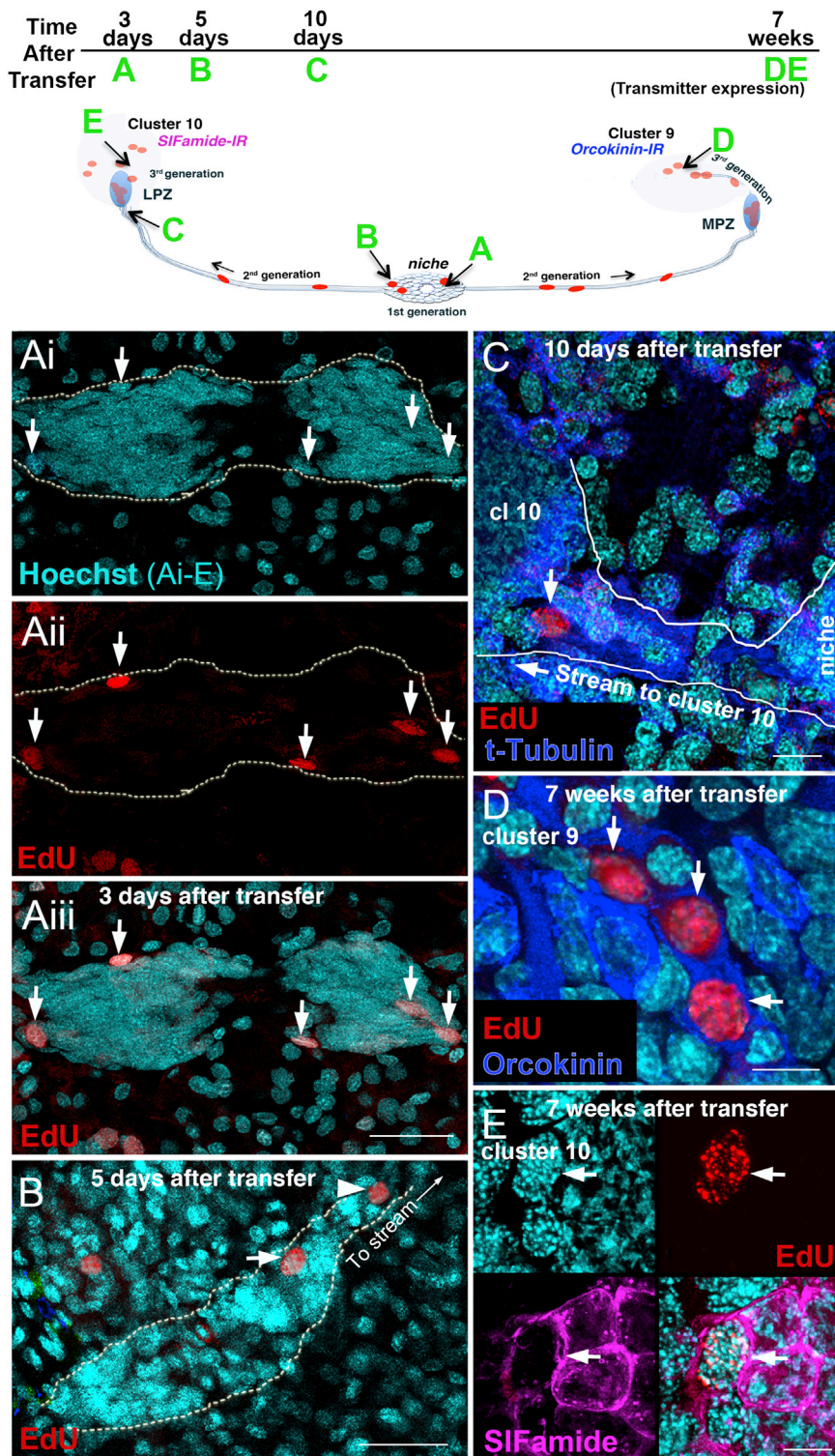
Adoptive Transfer of EdU-Labeled Hemocytes Results in the Appearance of Labeled Cells in the Niche, Streams, and Brain Clusters 9 and 10, Where They Express Appropriate Neurotransmitters

Prior in vitro studies have implicated hemocytes as a source of neuronal precursors supporting adult neurogenesis (Benton et al., 2011). The influences of r-AST1 on the niche (Figure 2), the effect of hematopoietic tissue ablations on the niche (Figure 3A), and the high correlations between THC and niche cell counts (Figures 3B and 3C) reinforce this theory. There-

Figure 5. EdU-Labeled Cells Are Observed in the Niche, Streams, and Clusters 9 and 10 of Recipient Crayfish after Adoptive Transfer of EdU-Labeled Hemocytes from Donor Animals

The schematic diagrams (top) illustrate the experimental timeline for each sample (time after transfer, A–E), and (bottom) the locations of the EdU-labeled cells that were observed. Images in (A), (B), and (D) are from *P. clarkii*; (C) and (E) are from *P. leniusculus*.

(A) Three days after adoptive transfer of hemocytes, EdU-labeled cells (red; arrows in Aii and Aiii) are observed in the niche (Ai). Hoechst 33342 (cyan) labels nucleic acids in all niche cells as well as nearby cells. The dashed line indicates the margins of the niche. Aiii shows the position of the EdU-labeled cells among the Hoechst labeling of the niche cells, with Hoechst (Ai) and EdU (Aii) separations and the merged images (Aiii). Scale bars represent 40 μm (Ai–Aiii).

(B) Five days after hemocyte transfer, EdU-labeled cells are again observed in the niche (arrow, B) and in the proximal regions of the streams near the niche (arrowhead, B). Scale bar represents 40 μm.

(C) Ten days after hemocyte transfer, cells are observed in the distal ends of the streams, near Cluster 9 and Cluster 10 (arrow points to an EdU-positive [red] cell). Immunoreactivity for t-tubulin (blue) highlights the niche and streams, which are also outlined. Scale bar represents 30 μm.

(D) Seven weeks after adoptive transfer of EdU-labeled hemocytes from donor to recipient crayfish, EdU-labeled cells (red) are observed in cell clusters 9 and 10. Some of these cells in Cluster 9 express orcokinin, a peptide transmitter used by many Cluster 9 cells. Scale bar represents 10 μm.

(E) Seven weeks after transfer of EdU-labeled hemocytes, EdU-labeled cells in Cluster 10 are immunoreactive for SIFamide, a transmitter of Cluster 10 neurons. E shows the separate channels for each fluorophore as well as the merged images (lower right). Scale bar represents 10 μm.

EdU-labeled cells have acquired properties typical of differentiated neurons in these regions (Sullivan et al., 2007; Kim et al., 2014). Following adoptive transfer of labeled hemocytes, EdU-labeled cells were not incorporated into other rapidly proliferating tissues such as hepatopancreas or the hematopoietic organ, indicating that the attraction of these cells to the niche and their progression through the neurogenic lineage is a specific, localized result.

As an additional control for the specificity of these interactions, cells from the hepatopancreas were labeled in donor crayfish and transferred to recipients using the same methods as for hemocytes. However, no labeled cells were observed in the neurogenic niche, streams, or brain cell clusters following these transfers. This demonstrates that incorporation of EdU into neuronal precursors in recipient animals is not a general outcome of cell transfers, but rather is a result specific to hemocytes, which argues against cell fusion events as a basis for our findings.
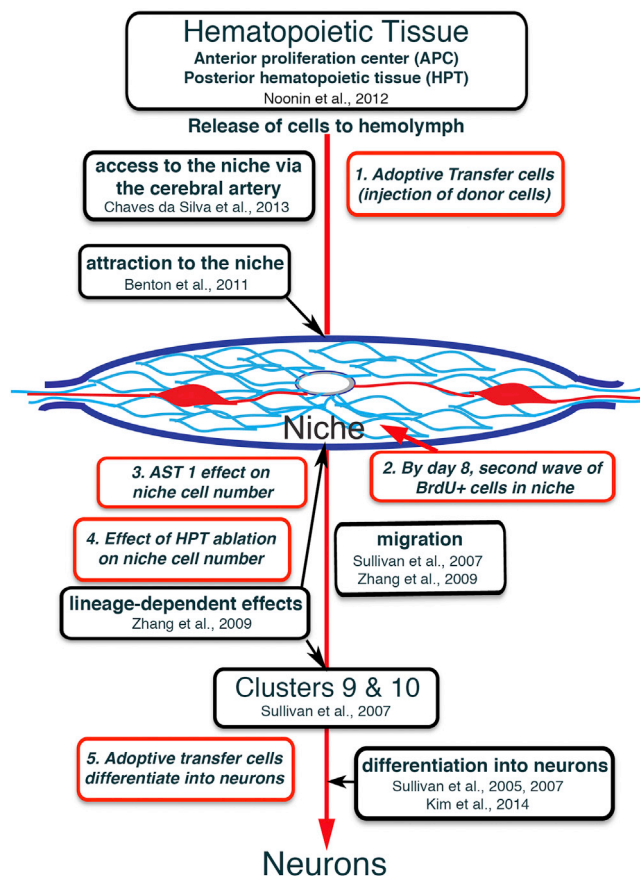
Figure 6. Current Model of Hematopoietic and Niche Cell Relationships

Based on our experimental data, we propose that the niche cells are derived from cells produced and released by hematopoietic tissues. These circulating hemocytes access the niche via the circulation and are attracted to the niche at least in part by serotonergic mechanisms. The daughters of the first-generation neuronal precursors migrate along streams and during this migration they undergo lineage-dependent influences before arriving at Clusters 9 and 10, where they differentiate into neurons. The current article contributes to our understanding of the role of the hematopoietic system in this process (items in red boxes). Previously published studies relevant to aspects of this model are cited.

DISCUSSION

Regulation of Adult Neurogenesis by the Innate Immune System

These studies demonstrate a close and direct relationship between the innate immune system and mechanisms of adult neurogenesis in the crustacean brain (Figure 6). First, the immune system regulates the neuronal precursor lineage through the release of AST1, which promotes the release of hemocytes from hematopoietic tissues and also increases niche cell numbers and the rate of BrdU incorporation into cells in the niche and streams. Second, total hemocyte counts are positively correlated with the numbers of cells composing the neurogenic niche; manipulation of circulating hemocyte levels results in highly predictable changes in the number of niche cells. These data show that the neurogenic niche is dynamically regulated by the immune system.

The Pool of First-Generation Neuronal Precursors in the Niche Must Be Replenished

The first-generation neuronal precursors in the adult crayfish brain are not self renewing and yet these are never exhausted throughout the long lives of these animals (Benton et al., 2011, 2013). We therefore concluded that the niche is not a closed system, and the pool of neuronal precursors must be replenished from a source extrinsic to the niche. The niche lies on a blood vessel and communicates with the circulation, but is otherwise physically isolated (Sullivan et al., 2007). For this reason, we tested the interaction between hemocytes and the niche in vitro and discovered that hemocytes (but not other cell types tested) are attracted to the niche (Benton et al., 2011). These cells extend processes into the niche and within 6 hr of introduction to organ cultures are integrated among niche cells, becoming immunoreactive for the niche marker glutamine synthetase. Further, serotonin immunoreactivity lines the vascular cavity of the niche, and the attraction between hemocytes and the niche is eliminated by interfering with serotonergic functions. These experiments suggested that hemocytes may be attracted to the niche at least in part by a serotonergic signaling mechanism. Collectively, these data indicated that hemocytes might be one source of neuronal precursors responsible for adult neurogenesis in the crustacean brain.

Mind the Gap: Evidence for an Extrinsic Source of Neuronal Precursors

The current experiments confirm the presence of an extrinsic source of neuronal precursors by documenting BrdU labeling in niche cells long after the initial labeling period and BrdU clearing time. After a single injection of BrdU, labeling for this nucleoside in niche cells was observed in groups of crayfish at intervals over a 21 day period. In the first 4 days following injection, between one and five niche cells were intensely immunoreactive for BrdU, consistent with many prior studies (Sullivan et al., 2007; Song et al., 2009). However, by day 5 following BrdU injection, niches were devoid of BrdU immunoreactivity, as shown previously. The present data demonstrate that following this "gap" in BrdU labeling, intensely labeled cells were once again observed in the niche, 8 days after the original injection of BrdU. This is precisely what would be expected if the turnover in the source tissue(s), release and travel time to the niche are taken into account. Given that the BrdU had long since cleared from the system, no new incorporation of BrdU was possible after the gap in labeling. Further, all of the original BrdU-labeled cells had divided and migrated away from the niche toward brain cell clusters 9 and 10 (Benton et al., 2011). We therefore conclude that BrdU was incorporated into these late-appearing BrdU+ cells while in their source tissue(s), during the initial labeling period following BrdU injection on "day 0." Further, the period between "day 0" and the second peak (days 8–14) is indicative of the time that must be necessary for the source-labeled cells to complete their lineage in the source tissue, mature and be released, and become integrated into the niche. In addition, the length of the second peak is likely to reflect the turnover time of the cell population in the source tissue.

Hemocytes Produce Differentiated Neurons

When hemocytes labeled with EdU in donor crayfish were transferred to recipient crayfish, labeled cells rapidly populated the

neurogenic niche, even though the labeled donor cells composed fewer than 1% of the circulating hemocytes. Further, cells containing nucleoside label were observed in the migratory streams, the normal route by which second-generation neuronal precursors travel from the niche to brain cell clusters 9 and 10. By 7 weeks after transfer, EdU-labeled cells were found in cell clusters 9 and 10, and these cells expressed the transmitter substances that are characteristic of these cell types. Hepatopancreas cells, labeled and transferred using the same methods as hemocytes, show none of these features. The current experiments demonstrate that cells harvested from the circulation and transferred directly to a recipient can become neuronal precursors.

Prior studies have demonstrated that thymidine analogs from grafted cells can be transferred into dividing host cells, including neural precursors, in vivo (Burns et al., 2006). Other studies have shown that cell fusion events (e.g., phagocytosis) can underlie translocation of the label from a transferred cell to a cell in a recipient animal (Coyne et al., 2006). We believe that the results of hemocyte transfers in crayfish are not subject to these same concerns for several reasons. First, the transferred cells are injected as live cells into the circulation of host crayfish. This does not involve surgery or grafting, as in prior studies and therefore may provoke less inflammatory response. Nevertheless, assuming that some transferred cells do die and release their contents, these are in such small numbers compared with the circulating hemocytes and blood volume of the host crayfish (see Experimental Procedures), that it is unlikely the release of nucleoside could be incorporated into other dividing cells in sufficient quantities to result in an effective label. If phagocytosis was involved, then cytoplasmic labeling (but not nuclear labeling) might be expected.

Our studies involve the attraction of the transferred cells to the neurogenic niche, a process that is likely to be highly selective. Consistent with this assumption, transfer of labeled hepatopancreas cells into recipient crayfish does not result in any labeled cells in the niche, migratory streams or brain cell clusters. This demonstrates both that the nucleoside is not transferred from donor cells to host cells and that the attraction to the niche is not a general property of transferred cells. Conversely, transferred hemocytes are not incorporated into hepatopancreas or hematopoietic tissues, although these tissues are rapidly proliferating, also suggesting that the interaction of donor hemocytes with the niche involves a specific attraction. Finally, the progression of transferred labeled hemocytes through the neuronal lineage to a differentiated neuronal phenotype involves many levels of engagement. These include signaling pathways underlying attraction to the niche (e.g., serotonin) (Benton et al., 2011; Zhang et al., 2011), specific migratory mechanisms (e.g., nucleokinesis) (Zhang et al., 2009), and expression of genes coding for appropriate neurotransmitters (e.g., orcokinin [Cluster 9 cells]; SIFamide [Cluster 10 cells]) (Sullivan et al., 2007). Our experiments therefore suggest that hemocytes are competent to become neuronal precursors and that these successfully respond to this sophisticated series of challenges.

CONCLUSIONS

These data are in contrast to models of stem cell generation in mammals that propose the capability of long-term self-renewal. The first-generation neuronal precursors residing in the crayfish brain, which are functionally analogous to neural stem cells in mammals, are not self-renewing. Three types of experiments support this claim. First, the first-generation neuronal precursors in the niche do not retain nucleoside labels (Benton et al., 2011). This is also clear in the current experiments where the timeline of niche cell labeling following a single BrdU pulse is plotted and a gap in BrdU labeling occurs (Figure 4). Second, cells in the niche undergo geometrically symmetrical divisions, and pairs of cells stay together as they begin to traverse the streams, also suggesting that both daughters migrate from the niche (Zhang et al., 2009). Third, the size of the labeled niche cell pool following increasing incubation times in BrdU (6 hr–10 days) was documented; if divisions are self-renewing (as in embryos), one might expect increasing numbers of BrdU-labeled cells in the niche with increasing incubation times, provided that the speed of migration is relatively slow (as indicated by our double-nucleoside labeling studies). However, no more than four cells were found in the niche regardless of BrdU incubation time (Benton et al., 2011). These three types of data therefore all indicate a lack of self-renewal among the first-generation neuronal precursors in the niche.

Prevailing thought also suggests that cells derived from one embryonic germ layer do not normally contribute to tissues originating from a different germ layer (transdetermination or transdifferentiation). However, our studies indicate that cells from the innate immune system can be a source of neuronal precursors in the adult brain, i.e., that cells derived from mesodermal tissues contribute to an organ that forms embryonically from ectoderm. Indeed, there is strong evidence that adult stem cells can contribute progeny to tissues originally derived from nonmesodermal germ layers. Adoptive transfer experiments in rodents and humans show that mesenchymal stem cells are capable of differentiating not only into a variety of mesodermal cell types, but also into neurons in the adult brain (Brazelton et al., 2000; Mezey et al., 2000, 2003). Thus it was concluded, "…bone marrow can make brain…" (Cogle et al., 2004). However, this interpretation was tempered by later work suggesting that the neuronal phenotype may have been induced by secreted factors or resulted from cell fusion, rather than from natural physiological mechanisms (for review, see Maltman et al., 2011; Mezey, 2011). The belief that neural stem cells undergo long-term self-renewal, and thus do not need to be replenished, has also influenced the perceived significance of the original findings. However, in the crustacean brain, where the first-generation neuronal precursors do not self-renew, a source of neural stem cells is necessary to replenish the pool of first-generation neuronal precursors in the niche. Considering the results cited here and our previously published work, it is likely that hemocytes are a natural source of first-generation neuronal precursors supporting adult neurogenesis in the crayfish brain. The current studies therefore suggest that one point of intersection between the immune system and nervous system may lie in the stem cell niche that supports adult neurogenesis.

EXPERIMENTAL PROCEDURES

Animals

Experiments were conducted using the freshwater crayfish (*Procambarus clarkii*) maintained in the Animal Care Facility at Wellesley College. Crayfish

were kept at room temperature on a 12/12 light/dark cycle in aquaria containing artificial pond water (double-distilled water with added trace minerals and sodium bicarbonate as a buffer). Adoptive transfer studies also were done at Uppsala University using *Pacifastacus leniusculus* housed in groups in large tanks with running fresh pond water and a 15/9 light/dark cycle.

Astakine Injection

Recombinant-AST1 (r-AST1) was generated in the laboratory of I.S. using an *Escherichia coli* expression system, as described in Lin et al. (2010). Crayfish (15–25 g; 17–20 mm carapace length [CL]) were injected at 18:30 with r-AST1 (Trx-S tag-astakine 1; 0.05 μg/g animal weight in crayfish saline: 205 mM NaCl, 5.4 mM KCl, 34.4 mM CaCl$_2$, 1.2 mM MgCl$_2$, and 2.4 mM NaHCO$_3$).

Total Hemocyte Counts following Astakine Injection

Hemolymph samples were taken from crayfish at 6, 12, 18, 24, and 48 hr after R-AST1 injection. Hemolymph was drawn from the dorsal sinus or from the base of the leg using a 1 ml syringe and diluted 1:2 with a cold anticoagulant solution of citrate buffer/EDTA (NaCl 0.14 M, glucose 0.1 M, trisodium citrate 30 mM, citric acid 26 mM, EDTA 10 mM, pH 4.6). Blood samples were mixed with 0.4% Trypan Blue solution and transferred to a hemocytometer for quantitative assessment (Figure 2A).

Niche Cell Counts and Quantitative Assessment of the Neuronal Precursor Cell Lineage

Crayfish (17–20 mm CL) were separated into three groups: controls, sham-injected, and r-AST1-injected. R-AST1 was injected as described above, and shams were injected with the same volume of crayfish saline. Crayfish were maintained in pond water with 5-bromo-2′-deoxyuridine (BrdU; 2 mg/ml; Sigma, B5002) for 24, 48, or 72 hr. Following dissection and fixation, standard immunocytochemical methods were used. Confocal images of the brains were used to count PI (or DAPI)-stained cells in the niche and BrdU-labeled profiles in the niche, streams, and cell clusters 9 and 10.

Total Niche Cell Counts

All cells labeled for both glutamine synthetase (GS) and either PI or DAPI (nuclear stains) in the region of the niche were considered "niche cells" and were included in the niche cell counts. If a cell was labeled with PI or DAPI without GS label, this was excluded from the counts.

BrdU-Labeled Cell Counts

The numbers of BrdU-labeled cells in the niche, migratory streams, and proliferation zones in Clusters 9 and 10 were counted blindly by individual observers. A single optical section was projected onto the monitor and the labeled cells traced onto a single transparent sheet. This was repeated for each optical section and the cell profiles then counted from the sheet.

Immunohistochemistry

Brains were dissected, fixed overnight in 4% paraformaldehyde in 0.1 M phosphate buffer (PB; 20 mM NaH$_2$PO$_4$, 80 mM Na$_2$HPO$_4$; pH 7.4), and processed using standard immunohistochemical methods as described in Zhang et al. (2009). The following primary antibodies were used: rat anti-BrdU (1:50; Accurate Chemical); anti-glutamine synthetase (GS; 1:100; BD Biosciences); anti-tyrosinated tubulin (1:1000; Sigma-Aldrich). The complimentary secondary antibodies (Jackson ImmunoResearch Laboratories) were goat anti-rat IgG-CY2 or CY3 (to detect BrdU); goat-anti-mouse IgG-Cy5 (for GS). After rinsing, brains were stained with the nucleic acid marker PI (1:100, Sigma) or DAPI (4′,6-diamidino-2-phenylindole; Molecular Probes) and mounted using Fluoro-Gel (Electron Microscopy Sciences).

Hematopoietic Tissue Ablations

Four groups of crayfish (20–25 mm CL) were assessed: control, sham, half-ablation (HA), and HA plus r-AST1. All crayfish except controls were placed on ice for 20 min prior to, and during, the procedure. A rotary drill (Dremel Tools) was used to make an incision in the dorsal cephalothorax, which was removed, and the posterior HPT exposed. For the HA and HA plus r-AST1 groups, an incision was made on one side, 1 mm from the dorsal median artery, and the HPT was teased away and removed. For the sham group, the dorsal cephalothorax was removed and the HPT was exposed (but untouched) for ~5 min, the time required to remove the HPT in the ablated

animals. The outer carapace was reattached by melting dental wax over the incision site, and animals were returned to tanks.

All animals were injected with BrdU (0.5 ml of 5 mg/ml BrdU) 5 days after surgery, 48 hr prior to sacrifice. The HA + AST1 group was injected 48 hr prior to sacrifice with 0.5 ml of 5 mg/ml BrdU and r-AST1 (0.05 μg/g animal weight in crayfish saline). All crayfish were killed on day 7 after surgery.

In order to correlate THC and niche cell numbers in crayfish after HPT manipulations, sham (n = 4) and HPT-ablated (n = 7) crayfish (18–20 mm CL) were prepared as described above. Hemolymph samples were taken 24 hr prior to animal sacrifice and hemocyte counts were determined. After killing the crayfish, brains were dissected, fixed, and processed immunocytochemically for GS and stained with PI, and THC and niche cell counts were performed.

As a control for the health of the crayfish following hematopoietic ablations, BrdU incorporation into the hepatopancreas was assessed. Hepatopancreas tissue was severed, processed for BrdU and PI, and then sliced into 10 μm sections using a Vibratome. Each piece of hepatopancreas is comprised of multiple bunches of hair-like fronds. BrdU labeling is confined to the lateral and anterior edges of these fronds. Because the fronds vary in size, the ratio between proliferating (BrdU and PI-labeled) and nonproliferating (PI-labeled only) cells was used. To determine the x and y axis counting limits, a line was drawn beneath the farthest posterior BrdU-labeled cell, as close to possible to a 90° angle from the tip of the frond. The z axis counting limits were determined by looking for the very first and last faint traces of the BrdU label in each piece of tissue.

BrdU Injection and Niche Analysis over 21 Days

BrdU (5 mg/ml) was injected into adult crayfish (30–35 mm CL). Groups of crayfish were sacrificed each day for the first week after injection and at intervals for the next 2 weeks. Brains and their associated niches were dissected and processed immunocytochemically for BrdU and GS (as above), stained with PI, mounted and examined with the confocal microscope.

Adoptive Transfer of Hemocytes

Donor crayfish (35–40 mm CL) were injected with 200–300 μl of EdU (0.02–0.2 mg/ml crayfish saline) and then returned to artificial pond water until hemolymph (200–300 μl) was withdrawn (3–5 days after EdU injection). Hemolymph was expelled from the syringe into an Eppendorf tube containing cold anticoagulant buffer (100–200 μl; NaCl, 0.14 M; EDTA, 10 mM; trisodium citrate, 30 mM; citric acid, 26 mM; glucose, 0.1 M; pH 4.6) and gently mixed. Using a new cold syringe and needle, 200 μl of solution containing labeled hemocytes was injected into recipient crayfish, which were then returned to their tanks. After dilution in the recipient hemolymph, <1% of circulating cells contained EdU label.

Recipient crayfish were killed between 3 days and 7 weeks after hemocyte transfers. Brains were dissected and processed with the ClickIt method for EdU detection and using standard immunocytochemical protocols (see above) for GS (*P. clarkii*) or t-tubulin (*P. leniusculus*) (and orcokinin and SIFamide for long-term transfers). Brains were stained with Hoechst 33342 and examined using the confocal microscope.

SIFamide and Orcokinin Antibody Specificities

To test for transmitter differentiation after long-term transfers, polyclonal rabbit anti-SIFamide (1:5,000; a gift from Dr. A. Yasuda) and polyclonal rabbit anti-orcokinin (1:5,000; a gift from Dr. H. Dircksen) were used. The rabbit anti-SIFamide antibody was raised against the SIFamide peptide (GYRKPPFNGSIFamide) conjugated to bovine serum albumin; staining with this antiserum in *P. clarkii* is colocalized with in situ hybridization for the mRNA for the same neuropeptide (Yasuda et al., 2004; Yasuda-Kamatani and Yasuda, 2006). The rabbit anti-orcokinin antibody was raised against a thyroglobulin conjugate of [ASN[13]] orcokinin (NFDEIDRSGFGFN; Bungart et al., 1994). All staining with this antiserum in the crayfish *Orconectes limosus* was abolished when the diluted antibody was preincubated with 50 nM of the immunizing peptide (Dircksen et al., 2000).

Confocal Microscopy

All imaging was done using a Leica TCS SP5 confocal microscope equipped with argon 488 nm and 561 and 633 nm diode lasers. Serial optical sections were taken at 0.5–1 μm intervals and saved as 3D stacks and 2D

projections. Image preparation and assembly were done in Photoshop 7 (Adobe Systems).

Data Analysis and Statistics

Data are presented as mean ±SEM. Comparisons between different groups of animals were made with Student's t tests (Figure 2A) or one-way ANOVA analysis followed by Tukey's multiple comparison tests (Figures 2B–2D, 3A, and S1) (JMP; SAS Institute).

SUPPLEMENTAL INFORMATION

Supplemental Information includes two figures and can be found with this article online at http://dx.doi.org/10.1016/j.devcel.2014.06.016.

AUTHOR CONTRIBUTIONS

ACKNOWLEDGMENTS

REFERENCES

An, C., Shi, Y., Li, P., Hu, X., Gan, Y., Stetler, R.A., Leak, R.K., Gao, Y., Sun, B.L., Zheng, P., and Chen, J. (2014). Molecular dialogs between the ischemic brain and the peripheral immune system: dualistic roles in injury and repair. Prog. Neurobiol. *115*, 6–24.

Beltz, B.S., Zhang, Y., Benton, J.L., and Sandeman, D.C. (2011). Adult neurogenesis in the decapod crustacean brain: a hematopoietic connection? Eur. J. Neurosci. *34*, 870–883.

Benton, J.L., Zhang, Y., Kirkhart, C.R., Sandeman, D.C., and Beltz, B.S. (2011). Primary neuronal precursors in adult crayfish brain: replenishment from a non-neuronal source. BMC Neurosci. *12*, 53.

Benton, J.L., Chaves da Silva, P.G., Sandeman, D.C., and Beltz, B.S. (2013). First-generation neuronal precursors in the crayfish brain are not self-renewing. Int. J. Dev. Neurosci. *31*, 657–666.

Brazelton, T.R., Rossi, F.M.V., Keshet, G.I., and Blau, H.M. (2000). From marrow to brain: expression of neuronal phenotypes in adult mice. Science *290*, 1775–1779.

Bungart, D., Dircksen, H., and Keller, R. (1994). Quantitative determination and distribution of the myotropic neuropeptide orcokinin in the nervous system of astacidean crustaceans. Peptides *15*, 393–400.

Burns, T.C., Ortiz-González, X.R., Gutiérrez-Pérez, M., Keene, C.D., Sharda, R., Demorest, Z.L., Jiang, Y., Nelson-Holte, M., Soriano, M., Nakagawa, Y., et al. (2006). Thymidine analogs are transferred from prelabeled donor to

host cells in the central nervous system after transplantation: a word of caution. Stem Cells *24*, 1121–1127.

Chaves da Silva, P.G., Benton, J.L., Beltz, B.S., and Allodi, S. (2012). Adult neurogenesis: ultrastructure of a neurogenic niche and neurovascular relationships. PLoS ONE *7*, e39267.

Chaves da Silva, P.G., Benton, J.L., Sandeman, D.C., and Beltz, B.S. (2013). Adult neurogenesis in the crayfish brain: the hematopoietic anterior proliferation center has direct access to the brain and stem cell niche. Stem Cells Dev. *22*, 1027–1041.

Cogle, C.R., Yachnis, A.T., Laywell, E.D., Zander, D.S., Wingard, J.R., Steindler, D.A., and Scott, E.W. (2004). Bone marrow transdifferentiation in brain after transplantation: a retrospective study. Lancet *363*, 1432–1437.

Coyne, T.M., Marcus, A.J., Woodbury, D., and Black, I.B. (2006). Marrow stromal cells transplanted to the adult brain are rejected by an inflammatory response and transfer donor labels to host neurons and glia. Stem Cells *24*, 2483–2492.

Dircksen, H., Burdzik, S., Sauter, A., and Keller, R. (2000). Two orcokinins and the novel octapeptide orcomyotropin in the hindgut of the crayfish Orconectes limosus: identified myostimulatory neuropeptides originating together in neurones of the terminal abdominal ganglion. J. Exp. Biol. *203*, 2807–2818.

Evans, I.R., Hu, N., Skaer, H., and Wood, W. (2010). Interdependence of macrophage migration and ventral nerve cord development in Drosophila embryos. Development *137*, 1625–1633.

Jiravanichpaisal, P., Söderhäll, K., and Söderhäll, I. (2004). Effect of water temperature on the immune response and infectivity pattern of white spot syndrome virus (WSSV) in freshwater crayfish. Fish Shellfish Immunol. *17*, 265–275.

Kim, Y.F., Sandeman, D.C., Benton, J.L., and Beltz, B.S. (2014). Birth, survival and differentiation of neurons in an adult crustacean brain. Dev. Neurobiol. *74*, 602–615.

Lin, X., Novotny, M., Söderhäll, K., and Söderhäll, I. (2010). Ancient cytokines, the role of astakines as hematopoietic growth factors. J. Biol. Chem. *285*, 28577–28586.

Makhijani, K., Alexander, B., Tanaka, T., Rulifson, E., and Brückner, K. (2011). The peripheral nervous system supports blood cell homing and survival in the *Drosophila* larva. Development *138*, 5379–5391.

Maltman, D.J., Hardy, S.A., and Przyborski, S.A. (2011). Role of mesenchymal stem cells in neurogenesis and nervous system repair. Neurochem. Int. *59*, 347–356.

Mezey, E. (2011). The therapeutic potential of bone marrow-derived stromal cells. J. Cell. Biochem. *112*, 2683–2687.

Mezey, E., Chandross, K.J., Harta, G., Maki, R.A., and McKercher, S.R. (2000). Turning blood into brain: cells bearing neuronal antigens generated *in vivo* from bone marrow. Science *290*, 1779–1782.

Mezey, E., Key, S., Vogelsang, G., Szalayova, I., Lange, G.D., and Crain, B. (2003). Transplanted bone marrow generates new neurons in human brains. Proc. Natl. Acad. Sci. USA *100*, 1364–1369.

Ng, K.L., Li, J.-D., Cheng, M.Y., Leslie, F.M., Lee, A.G., and Zhou, Q.-Y. (2005). Dependence of olfactory bulb neurogenesis on prokineticin 2 signaling. Science *308*, 1923–1927.

Noonin, C., Lin, X., Jiravanichpaisal, P., Söderhäll, K., and Söderhäll, I. (2012). Invertebrate hematopoiesis: an anterior proliferation center as a link between the hematopoietic tissue and the brain. Stem Cells Dev. *21*, 3173–3186.

Ransohoff, R.M., and Engelhardt, B. (2012). The anatomical and cellular basis of immune surveillance in the central nervous system. Nat. Rev. Immunol. *12*, 623–635.

Schmidt, M., and Harzsch, S. (1999). Comparative analysis of neurogenesis in the central olfactory pathway of adult decapod crustaceans by in vivo BrdU labeling. Biol. Bull. *196*, 127–136.

Sintoni, S., Benton, J.L., Beltz, B.S., Hansson, B.S., and Harzsch, S. (2012). Neurogenesis in the central olfactory pathway of adult decapod crustaceans: development of the neurogenic niche in the brains of procambarid crayfish. Neural Dev. *7*, 1.

Söderhäll, I., Bangyeekhun, E., Mayo, S., and Söderhäll, K. (2003). Hemocyte production and maturation in an invertebrate animal; proliferation and gene expression in hematopoietic stem cells of Pacifastacus leniusculus. Dev. Comp. Immunol. *27*, 661–672.

Söderhäll, I., Kim, Y.A., Jiravanichpaisal, P., Lee, S.Y., and Söderhäll, K. (2005). An ancient role for a prokineticin domain in invertebrate hematopoiesis. J. Immunol. *174*, 6153–6160.

Song, C.K., Johnstone, L.M., Edwards, D.H., Derby, C.D., and Schmidt, M. (2009). Cellular basis of neurogenesis in the brain of crayfish, *Procambarus clarkii*: Neurogenic complex in the olfactory midbrain from hatchlings to adults. Arthropod Struct. Dev. *38*, 339–360.

Stewart, J.E., Cornick, J.W., and Dingle, J.R. (1967). An electronic method for counting lobster (*Homarus americanus* Milne Edwards) hemocytes and the influence of diet on hemocyte numbers and hemolymph proteins. Can. J. Zool. *45*, 291–304.

Sullivan, J.M., and Beltz, B.S. (2005a). Newborn cells in the adult crayfish brain differentiate into distinct neuronal types. J. Neurobiol. *65*, 157–170.

Sullivan, J.M., and Beltz, B.S. (2005b). Integration and segregation of inputs to higher-order neuropils of the crayfish brain. J. Comp. Neurol. *481*, 118–126.

Sullivan, J.M., Benton, J.L., Sandeman, D.C., and Beltz, B.S. (2007). Adult neurogenesis: a common strategy across diverse species. J. Comp. Neurol. *500*, 574–584.

Vogt, G. (2002). Functional anatomy. In Biology of Freshwater Crayfish, D.M. Holdich, ed. (Oxford: Blackwell Science), pp. 53–151.

Watthanasurorot, A., Söderhäll, K., Jiravanichpaisal, P., and Söderhäll, I. (2011). An ancient cytokine, astakine, mediates circadian regulation of invertebrate hematopoiesis. Cell. Mol. Life Sci. *68*, 315–323.

Yamazaki, S., Ema, H., Karlsson, G., Yamaguchi, T., Miyoshi, H., Shioda, S., Taketo, M.M., Karlsson, S., Iwama, A., and Nakauchi, H. (2011). Nonmyelinating Schwann cells maintain hematopoietic stem cell hibernation in the bone marrow niche. Cell *147*, 1146–1158.

Yasuda, A., Yasuda-Kamatani, Y., Nozaki, M., and Nakajima, T. (2004). Identification of GYRKPPFNGSIFamide (crustacean-SIFamide) in the crayfish *Procambarus clarkii* by topological mass spectrometry analysis. Gen. Comp. Endocrinol. *135*, 391–400.

Yasuda-Kamatani, Y., and Yasuda, A. (2006). Characteristic expression patterns of allatostatin-like peptide, FMRFamide-related peptide, orcokinin, tachykinin-related peptide, and SIFamide in the olfactory system of crayfish *Procambarus clarkii*. J. Comp. Neurol. *496*, 135–147.

Zhang, Y., Allodi, S., Sandeman, D.C., and Beltz, B.S. (2009). Adult neurogenesis in the crayfish brain: proliferation, migration, and possible origin of precursor cells. Dev. Neurobiol. *69*, 415–436.

Zhang, Y., Benton, J.L., and Beltz, B.S. (2011). 5-HT receptors mediate lineage-dependent effects of serotonin on adult neurogenesis in Procambarus clarkii. Neural Dev. *6*, 2.